Investigation of Stress in MEMS Sensor Device Due to Hygroscopic and Viscoelastic Behavior of Molding Compound

Yeonsung Kim, Dapeng Liu, Hohyung Lee, Ruiyang Liu, Dipak Sengupta, and Seungbae Park

***Abstract*— The stresses due to moisture saturation on microelectromechanical systems (MEMS) sensor devices after exposure to temperature cycling have been addressed. Moisture-, temperature-, and time-dependent material property of molding compounds for the MEMS devices were characterized. To determine the coefficient of hygroscopic swelling of a molding compound and diffusivity (D) of water in the molding compound, dimensional change and weight loss of moisture saturated samples at various temperatures were monitored by the digital image correlation method combined with a weight scale. To obtain the viscoelastic property of the molding compound, a series of stress relaxation tests was performed using dynamic mechanical analysis (DMA). To explain the moisture-induced viscoelastic behavior, a simple assumption was introduced based on the temperature of glass transition point (T_g) shift from the DMA result. The experimental data were utilized in numerical simulations to estimate the temperature- and moisture-induced stress on MEMS sensor devices subjected to temperature cycles.**

***Index Terms*— Hygroscopic swelling coefficient, microelectromechanical systems (MEMS), moisture diffusion, molding compound, viscoelasticity.**

I. Introduction

RECENTLY, a large number of microelectromechanical systems (MEMS) sensor devices are being used in industrial, instrumentation, and vehicle safety and support systems. Many of these applications demand high-precision sensors in standard semiconductor packages regardless of the external environment such as temperature excursion and relative humidity (RH) change. However, epoxy-based molding compound, a major packaging material for many MEMS sensor devices, has mechanical and materials characteristics affected by temperature and moisture. Molding compound absorbs moisture and swells when it is exposed to a humid environment [1]. On the other hand, the silicon chips and lead frame are impermeable to moisture. This mismatch of the hygroscopic strain generates stresses at the interface between molding compound and chips as well as the lead frame. In addition, the discrepancy in the coefficient of thermal expansion (CTE) and modulus of dissimilar materials in the same package induces thermomechanical stresses to the sensor when the MEMS package is subjected to the reflow process or thermal cycles. If hygroscopic and thermomechanical stresses combine together during temperature cycling, it may result in a signal shift of the system's sensor because its structure is highly sensitive to stress. In severe cases, the delamination or catastrophic failure so-called popcorning might happen [2]. Therefore, it is important to know the hygroscopic and thermomechanical stresses of molding compound to assure the performance and reliability of MEMS sensor device.

The moisture sorption characteristic of molding compounds has been one of the critical issues in designing the electronics parts and predicting its reliability. In [17] and [19]–[21], moisture diffusion properties of polymeric material were experimentally investigated. Volumetric expansion of materials by moisture ingression can be defined by the coefficient of hygroscopic swelling (CHS) [1]. Many efforts have been devoted to measure the CHS of molding compounds throughout a wide temperature range [1], [3]–[5]. Zhou *et al.* [25], [27] and Zhou [26] have investigated the effect of nonuniform moisture distribution on CHS characterization. Park *et al.* [5] and Jang *et al.* [6] have demonstrated that digital image correlation (DIC) technique can be successfully adopted to determine molding compound CHS. To cope with the initial moisture loss of the sample, Kwak [7] developed a new DIC measurement setup eliminating a heating up process. The experimental data are used for analysis to estimate the moisture-induced strains and stresses. The moisture diffusion can be calculated by implementing the fundamental concepts of heat transfer and hygroscopic swelling strain can be treated as an additional thermal strain in simulation [4], [7], [12], [20], [23], [24], [28]. Some alternative approaches were also proposed. For example, one approach for ANSYS users is to use fluence, one type of body load that ANSYS software provides, to account for the swelling effect [12]. Fan and Zhao [28] studied the stress due to combined thermal, hygroscopic swelling, and vapor pressure loads using this method.

Viscoelasticity is a distinguishing characteristic of a material such as a polymer. It has two aspects involving the time and temperature dependencies. Due to this nature of molding

Manuscript received July 22, 2014; revised January 22, 2015; accepted May 27, 2015. Date of publication June 30, 2015; date of current version July 15, 2015. This work was supported by Analog Devices, Inc. Recommended for publication by Associate Editor J.-H. Zhao upon evaluation of reviewers' comments.

Y. Kim, D. Liu, H. Lee, R. Liu, and S. Park are with the Department of Mechanical Engineering, State University of New York at Binghamton, Binghamton, NY 13902-6000 USA (e-mail: ykim35@binghamton.edu; dliu5@binghamton.edu; hlee11@binghamton.edu; rliu8@binghamton.edu; sbpark@binghamton.edu).

D. Sengupta is with the Packaging and Assembly Group, Analog Devices, Inc., Wilmington, MA 01887 USA (e-mail: dipak.sengupta@analog.com).

Color versions of one or more of the figures in this paper are available online at http://ieeexplore.ieee.org.

Digital Object Identifier 10.1109/TCPMT.2015.2442751

compounds, the stress generated in the MEMS package is influenced by the temperature cooling rate [8]. Thus, the viscoelastic property should be taken into consideration in MEMS package simulations. In [9] and [10], viscoelasticity effects on MEMS were investigated in depth. Recently, a design optimization of an MEMS pressure sensor based on the hygroscopic stress of the packaging material was studied [11]. The moisture absorption of polymeric material undergoes changes that affect their mechanical performances. The relaxation point of the material shifts to lower temperatures, while increasing its water contents due to the plasticization effect, resulting in a temperature shift of the glass transition point (T_g) to lower temperatures [13]. The time–water content superposition was suggested to construct the master curve to explain the hygroviscoelastic behavior under the water environment [13]–[15]. Yoon *et al.* [12] presented a nonlinear analysis scheme to evaluate the integrated impact of thermal and hygroscopic deformations for polymeric materials. However, a rigorous investigation about the combined effect of both hygroscopic and viscoelastic characteristics of molding compound on MEMS has not been published.

The primary focus of this paper is to investigate the hygrothermoviscoelastic behavior of a molding compound and its impact on MEMS sensor device. To determine CHS of the molding compound and diffusivity (D) of water in the molding compound, the moisture soaking test was performed first. Then, the dimensional change and weight loss of moisture in the saturated samples at various temperatures were monitored by DIC method and a weight scale, respectively. To obtain a viscoelastic property of the molding compound, a series of stress relaxation tests was performed using dynamic mechanical analysis (DMA). 3-D finite element analysis (FEA) model was established based on the experimental results and the hygrothermally induced stress of MEMS sensor was predicted.

II. Theoretical Background

A. Moisture Diffusivity and CHS

The moisture diffusion of a polymeric material can be defined by Fick's second law, which is described by

$$\dot{C} = \nabla \cdot (D \nabla C) \tag{1}$$

where C is the moisture concentration (mg/mm^3) and D is the diffusivity (mm^2/s). For an isotropic material, the equation yields

$$\frac{\partial C}{\partial t} = D\left(\frac{\partial^2 C}{\partial x^2} + \frac{\partial^2 C}{\partial y^2} + \frac{\partial^2 C}{\partial z^2}\right). \tag{2}$$

The above equation can be solved using a standard separation of variable method for the rectangular block sample. It yields an expression for the local moisture concentration as a function of time, position, and diffusivity. However, it is impossible to measure the local moisture concentration gradient in the sample. Thus, the weight change of sample as a function of time measured by exposing a dry sample to a humid environment or drying out the moisture saturated sample. Then, an analytical solution for the weight gain or loss with respect to time can be obtained by integrating the local moisture concentration over the volume of the sample [17]. The moisture and saturated weight gains are defined as

$$w(t)(\text{in } \%\text{wt}) = \frac{W(t) - W_{\text{dry}}}{W_{\text{dry}}} \times 100 \tag{3}$$

$$w_{\text{sat}}(\text{in } \%\text{wt}) = \frac{W_{\text{sat}} - W_{\text{dry}}}{W_{\text{dry}}} \times 100 \tag{4}$$

where $W(t)$ is an instantaneous weight of sample. W_{sat} is the saturated weight and W_{dry} is the dried weight of sample, respectively. The analytical solution of Fickian diffusion is well reviewed in [16] and [21]. In case of the moisture loss, the analytical solution of (2) is expressed as

$$\frac{W(t)}{W_{\text{sat}}} = \frac{512}{\pi^6} \sum_{l=0}^{\infty} \sum_{m=0}^{\infty} \sum_{n=0}^{\infty} \frac{\exp\left(\frac{-Dt}{L_{\text{eqv}}^2}\right)}{(2l+1)^2(2m+1)^2(2n+1)^2} \tag{5}$$

where

$$L_{\text{eqv}}^2 = \left\{\left[\frac{(2l+1)\pi}{x_0}\right]^2 + \left[\frac{(2m+1)\pi}{y_0}\right]^2 + \left[\frac{(2n+1)\pi}{z_0}\right]^2\right\}^{-1}. \tag{6}$$

Here, L_{eqv} is an equivalent length scale, x_0, y_0, and z_0 are the length, width, and thickness dimensions, respectively [17]. The diffusivity is determined by the nonlinear regression fit of the experimental data and (5). The moisture concentration and saturated moisture concentration are defined by

$$C(t) = \frac{W(t) - W_{\text{dry}}}{V} \tag{7}$$

$$C_{\text{sat}} = \frac{W_{\text{sat}} - W_{\text{dry}}}{V} \tag{8}$$

where V is the volume of specimen. The relationship between diffusivity and temperature is known to follow the Arrhenius equation, which is expressed as

$$D = D_0 \exp\left(-\frac{Q}{RT}\right) \tag{9}$$

where D_0 is the diffusivity constant (mm^2/s), Q is the activation energy (J/mol), R is the universal gas constant (8.3145 J/molK), and T is the absolute temperature (K).

Hygroscopic strain can be defined as

$$\varepsilon_{\text{hygro}} = \beta C \tag{10}$$

where β is CHS (mm^3/mg). In case of desorption, the moisture concentration and hygroscopic strain of the saturated sample are measured in the isothermal condition with respect to time. The linear relationship between the hygroscopic strain and moisture concentration can be defined as CHS [4].

B. Viscoelasticity

Molding compound has a dual nature of material characteristics, which exhibits both elastic and viscous behaviors. While the elastic response is instantaneous, the viscous response occurs over time. Due to this viscous characteristic, the molding compound shows a time-dependent behavior. It has been presented that the MEMS sensor signal

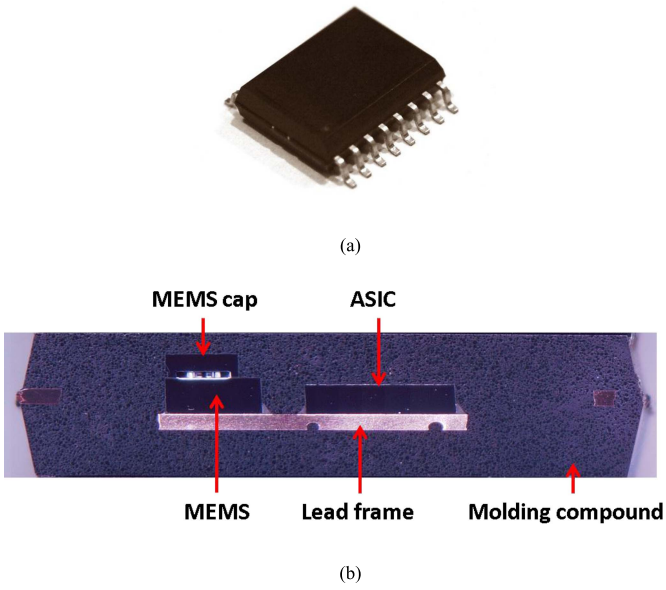

(a)

(b)

Fig. 1. Sixteen lead SOIC MEMS package. (a) Package image. (b) Cross-sectional image.

is very susceptible to the temperature cooling rate during assembly process [8]. The stress relaxation test is performed to characterize this time- and temperature-dependent material property. The constant strain is applied on the sample and stress change is monitored for a certain time. In addition, this test is repeated under various temperatures. With the assumption of simple thermorheological behavior of the mold compound, a master curve is constructed by shifting a series of relaxation curves at different temperatures from the reference temperature along the log time scale axis [18]. The master curve is fitted with Prony series, which is expressed as

$$E(t) = \frac{\sigma(t)}{\varepsilon_0} = E_\infty + \sum_{i=1}^{n} E_i \exp\left(-\frac{t}{\tau_i}\right), \quad \tau_i = \frac{\eta_i}{E_i} \tag{11}$$

where $E(t)$ is the relaxation modulus, $\sigma(t)$ is the stress as a function of time, ε_0 is the constant strain, and E_∞ is a fully relaxed modulus. Here, E_i and τ_i are referred to be a Prony pair, which is employed to describe the viscoelasticity in many FEA software. E_i is the elastic modulus, η_i is the viscosity, and τ_i is the relaxation time of ith Prony pair.

The shift distance of curves at various temperatures used to construct the master curve is fitted with the shift function. Williams–Landel–Ferry (WLF) equation is one of the most common shift functions and is written as

$$\log \alpha_T = -\frac{C_1(T - T_0)}{C_2 + (T - T_0)} \tag{12}$$

where $\log \alpha_T$ is the shift distance. C_1 and C_2 are constants. T_0 is the reference temperature.

III. Experiment

A. Specimens

Fig. 1 shows the MEMS sensor package studied in this paper. The package is 16 lead small outline integrated circuit (SOIC) type, which has body dimensions of 10.0 mm × 7.5 mm × 2.3 mm (except lead frame). It has an MEMS sensor die and ASIC die. Both the dies are mounted on to a lead frame using a die attach adhesive. Then they are wire bonded and encapsulated by the molding compound, which is cured at 175 °C. The condition of post mold cure (PMC) process is 4 h at 175 °C. The dimensions of the MEMS die is 1.8 mm × 1.6 mm × 0.6 mm and the ASIC die is 2.5 mm × 2.5 mm × 0.5 mm. The MEMS die has a cap to protect the MEMS structure, which is attached with seal glass. The dimension of the cap is 1.8 mm × 1.24 mm × 0.4 mm. The thicknesses of die attach adhesive, lead frame, and seal glass are 0.02, 0.26, and 0.02 mm, respectively. The specimen is an inverted type package to avoid electromagnetic interference. Thus, MEMS and ASIC are facing the board side in Fig. 1(b).

For property measurement purposes, the molding compound was fabricated into a bar shape. The same PMC condition of assembly process was applied after fabrication. For the moisture diffusivity and hygroscopic strain measurement, the bar samples were cut and polished to dimensions of 10 mm × 10 mm × 1.6 mm ($L \times W \times T$). The sample variation was ±0.05 mm. The specimen dimensions for the stress relaxation test were 30 mm × 13.14 mm × 0.87 mm ($L \times W \times T$). The die attach adhesive samples were also built for CTE and relaxation modulus measurement with dimensions of 30 mm × 8.73 mm × 0.98 mm ($L \times W \times T$).

B. Moisture Weight Loss, Hygroscopic Strain, and CTE Measurement

In this paper, the diffusivity of desorption was characterized in order to investigate the stress of the moisture saturated MEMS component exposed to thermal cycling. Accordingly, observations were concluded on the hygroscopic shrinkage of the moisture saturated sample after exposure to high temperatures. Although the die attach adhesive is also permeable to water, the molding compound was assumed to be an only material influenced by moisture in this paper. Since experimental results from material property characterization showed that the modulus of molding compound was much higher (more than ×20) than that of die attach adhesive, the hygroscopic stress and strain generated from molding compound may be dominant. Moreover, a majority of the package volume is comprised of mold compound. Therefore, the stress change of MEMS due to hygroscopic stress and strain from die attach adhesive can be neglected.

To determine the time required to achieve full saturation condition, four molding compound samples were dried at 120 °C for 72 h and placed in an environmental chamber controlled to 85 °C and 85% RH. The weight of each sample was periodically monitored using a high precision electronic scale until the fully saturated condition was achieved. The resolution of the scale was 0.01 mg. Fig. 2 shows the weight gain with respect to time. The results indicate that samples need to be placed in an environmental chamber with 85 °C/85% RH for 84 h to achieve full saturation. These conditions were applied to additional samples, some which

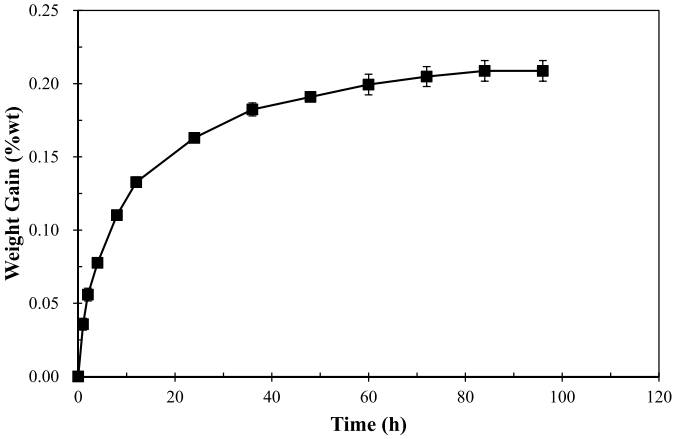

Fig. 2. Moisture absorption plot with respect to time.

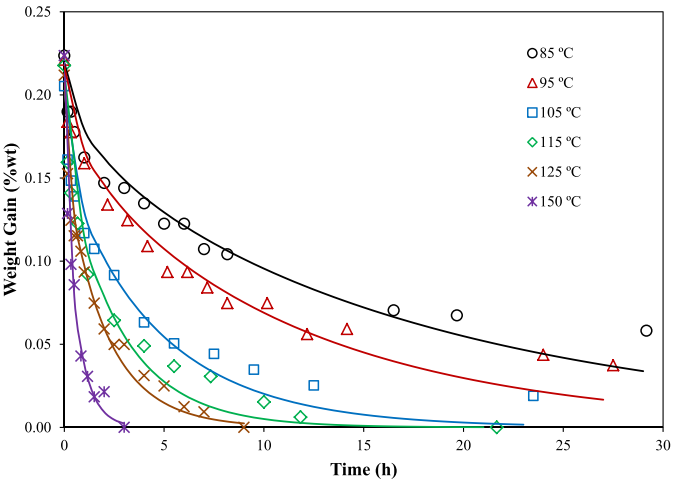

Fig. 3. Moisture weight gain (bullets) and Fickian curves (lines) of moisture desorption test under various temperatures.

were used for measuring moisture diffusivity and others for measuring hygroscopic strain.

To characterize the moisture diffusivity, the saturated specimens were placed in the preheated oven with the isothermal conditions: 85 °C, 95 °C, 105 °C, 115 °C, 125 °C, and 150 °C. To observe the weight loss, the specimen was taken out of the chamber and placed on the high precision electronic scale. After the measurement, the specimen was placed back into the chamber. The error due to this measurement procedure and reheating of sample when it was placed back into the oven can be negligible [19]. Each sample was measured at each temperature point. The experimental data of the weight loss with respect to time are plotted in Fig. 3. The solid lines represent the analytical Fickian fit (3) deduced by the nonlinear regression method. The result shows the discrepancy between Fickian fit and experimental data in the later stage of test, especially in low temperatures. The moisture weight gain is almost constant at the later stages of exposure. It might be attributed to the imperfect drying condition at low temperatures [19]. Fig. 4 shows the Arrhenius fit of measured diffusivity constant at each temperature. The results follow the Arrhenius relationship well.

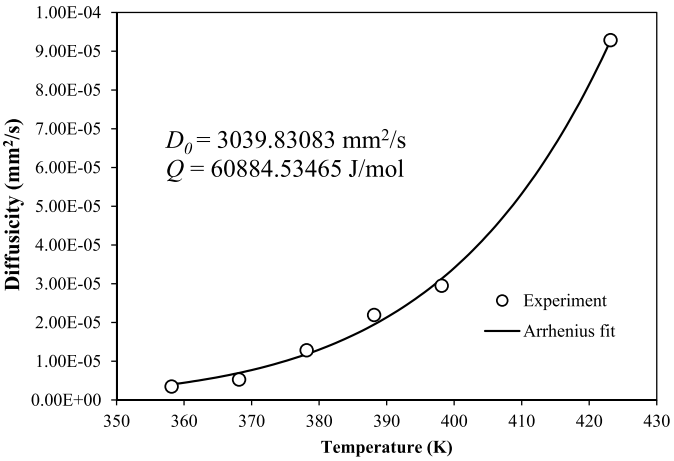

Fig. 4. Arrhenius curve.

DIC, which is a form of photogrammetry, is a noncontact full-field optical measurement technique in which both the in-plane and out-of-plane displacements can be computed by the pictures of the target object at the initial and deformed stage [22]. This is attained by correlating thousands of identical pixels (facets) on the object of measurement, which are considered as strain gauges. Implementation of DIC technique for CHS measurement has been well established [5], [6]. Unlike other conventional techniques, such as thermomechanical analyzer (TMA), the full-filed deformation of the specimen can be obtained by DIC. Therefore, the local strain variation in the sample due to the spatial property deviation can be removed. On the other hand, TMA only measures the deformation in a limited area of the sample where the probe is located, which might result in misinterpretation of strain. Another technical challenge of the CHS measurement using TMA and thermogravimetric analysis is the moisture loss during ramp up temperature prior to measuring. Thus, the DIC method, with preheated chamber proposed in [7], was implemented in this paper. In this method, the specimens of identical dimension were placed in the preheated chambers. The deformation measurement by DIC and weight loss measurement were performed simultaneously. Thereby, the technical challenges previously mentioned can be effectively minimized. DIC setup is shown in Fig. 5. The white speckles were applied on the specimen surface by a spray to generate facet before they were placed in the oven to dry.

The saturated specimen was placed in a preheated oven and the in-plane deformation of its surface was captured. After placing in the preheated chamber, the specimen expanded until it reached to the isothermal temperature. Then, it started to shrink due to moisture loss. Typically, it takes about 1–2 min and this initial expansion was not included in CHS calculation. After this initial expansion, the image was captured every 5 min. Then, the hygroscopic strain was calculated by DIC analysis. Like the weight loss measurement, each sample was tested at each temperature. The resolution of the strain measurement was ±0.004%. The hygroscopic strain with respect to time during moisture desorption process is plotted in Fig. 6. Based on the test results of weight loss and the strain measurement, the hygroscopic strains as a function of

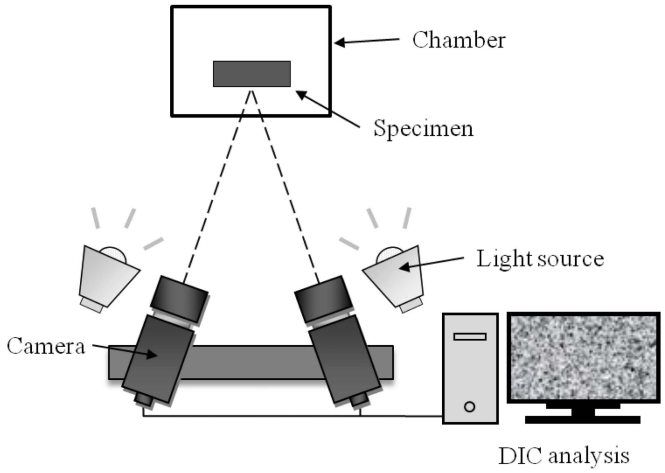

Fig. 5. Schematic of DIC system setup.

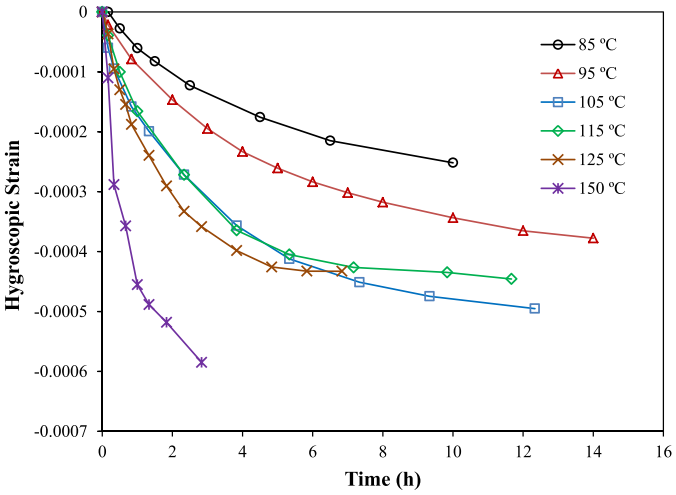

Fig. 6. Hygroscopic strain at various temperatures.

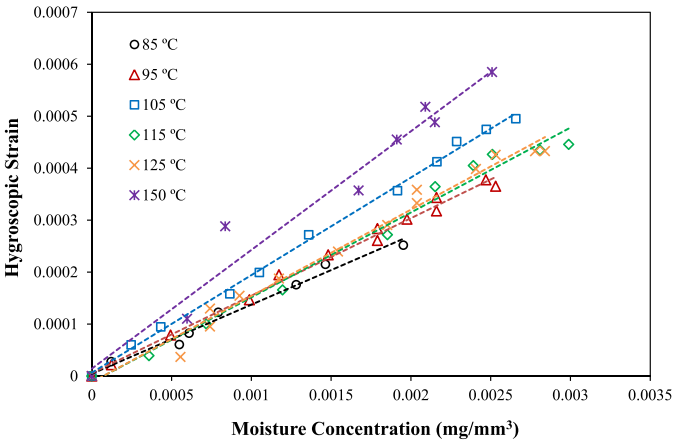

Fig. 7. CHS at various temperatures.

moisture concentration were calculated and plotted in Fig. 7. The corresponding CHS is listed in Table I. The results show that as temperature increases, CHS also increases. This trend is more significant above the glass transitions phase. As shown in Fig. 6, the hygroscopic strain at 105 °C is higher than that at 115 °C and 125 °C, so the CHS at 105 °C exhibits a sudden increase. It might be attributed to an abrupt material property change near T_g.

TABLE I
DIFFUSIVITY AND CHS

Temperature (°C)	D (mm^2/s)	CHS (mm^3/mg)
85	3.46E-06	0.133
95	5.28E-06	0.149
105	1.28E-05	0.188
115	2.19E-05	0.163
125	2.95E-05	0.166
150	9.29E-05	0.228

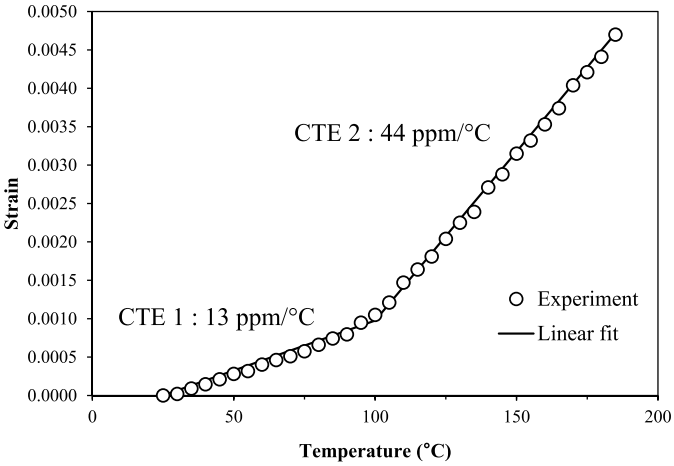

(a)

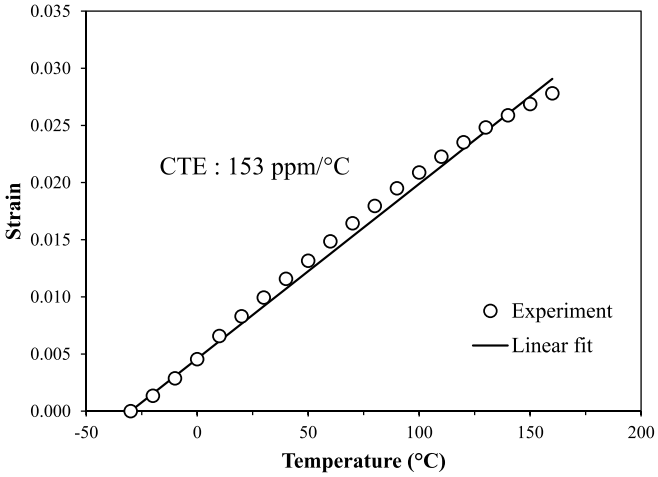

(b)

Fig. 8. CTE measurement result. (a) Molding compound. (b) Die attach adhesive.

In addition, the CTE of dried specimen was characterized using DIC. By measuring the in-plane deformation of the specimen during temperature increase, the material strain in terms of temperature can be obtained. CTE is determined by the linear slope of a function between the in-plane deformation and temperature. Fig. 8(a) shows the in-plane strain measurement results and the CTE. Similarly, the CTE of the die attach adhesive was also characterized by DIC and plotted in Fig. 8(b).

C. Stress Relaxation Test

DMA was utilized to evaluate the relaxation modulus. A series of stress relaxation tests has been executed for dried molding compounds in the three point bending tests at

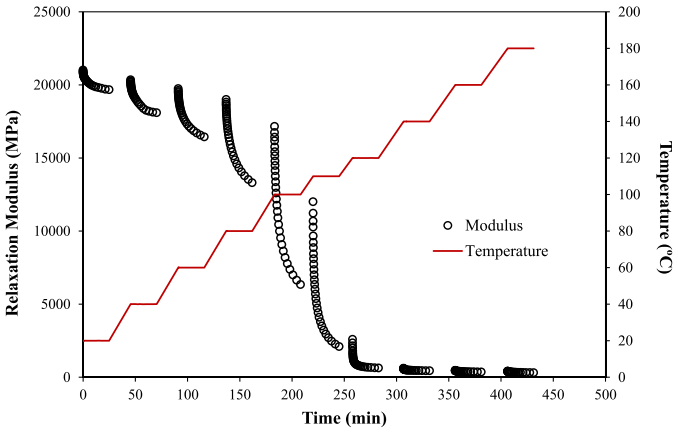

Fig. 9. Stress relaxation result of the molding compound.

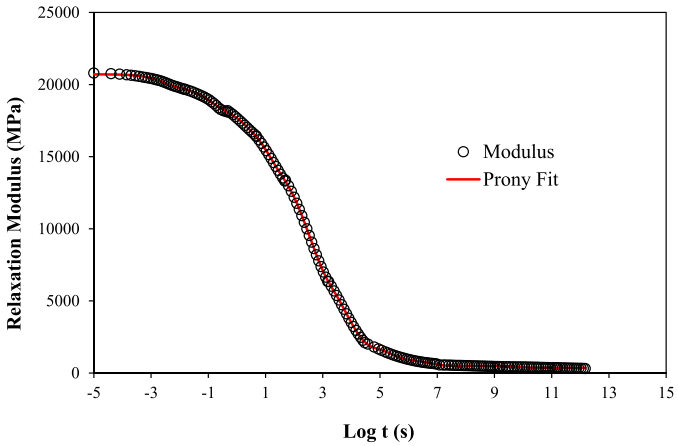

(a)

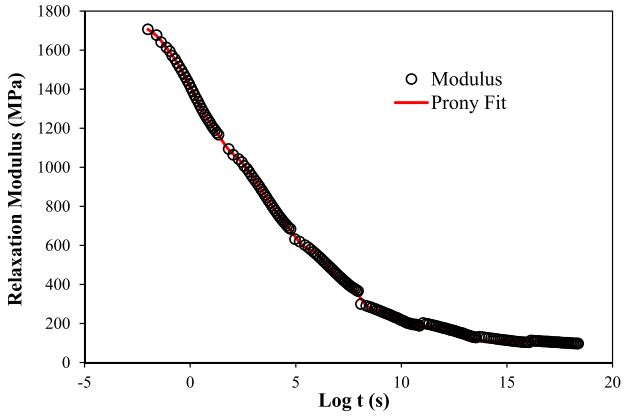

(b)

Fig. 10. Master curve. (a) Molding compound. (b) Die attach adhesive.

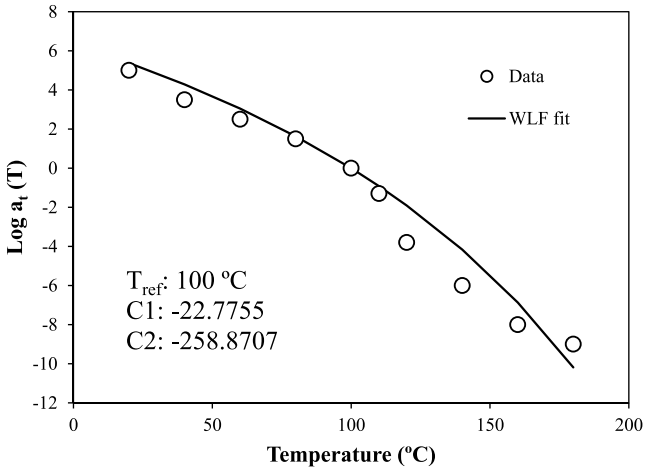

(a)

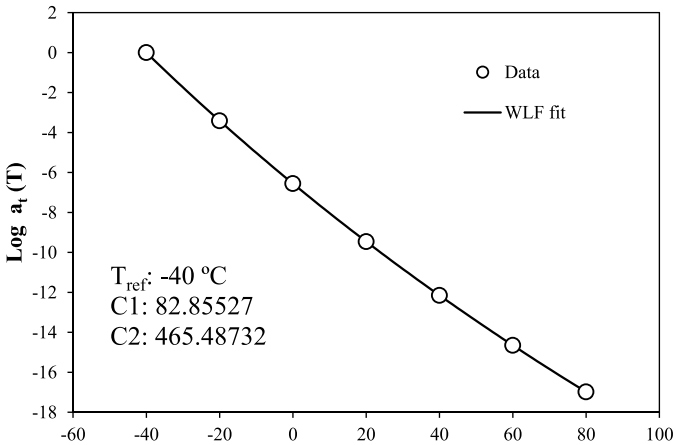

(b)

Fig. 11. Shift distance and WLF fit. (a) Molding compound. (b) Die attach adhesive.

TABLE II
PRONY PAIRS OF THE MOLDING COMPOUND

i	E_i/E_0	τ_i
1	0.040086	0.00284
2	0.061685	0.09544
3	0.051816	1.07389
4	0.137576	10.97108
5	0.107145	104.67782
6	0.121312	434.37762
7	0.120439	434.73504
8	0.101512	3065.44095
9	0.164514	12118.43676
10	0.047320	259531.7945
11	0.022634	6074150
12	0.006793	8875370000
E_0 (MPa)	20712.96263	

various temperatures. The span length was 20 mm. The test was conducted at every 20 °C from 20 °C to 180 °C. The temperature increase rate was 5 °C/min. After 5 min, for the temperature stabilization, a constant strain of 0.1% of the span length was applied for 25 min, followed by 10-min recovery time. The stress relaxation test result is shown in Fig. 9 and the established master curves are plotted in Fig. 10. The shift distance and the WLF shift fit are shown in Fig. 11. In addition, the relaxation modulus of die attach adhesive was characterized with the identical condition in the temperature range from −40 °C to 80 °C. The master curve and shift fit are plotted in Figs. 10 and 11. The Prony pairs are listed in Tables II and III. E_0 is the instantaneous modulus when time is zero.

TABLE III
PRONY PAIRS OF THE DIE ATTACH ADHESIVE

i	E_i/E_0	τ_i
1	0.057977	0.04066
2	0.084608	0.33913
3	0.120664	2.36345
4	0.102022	24.90482
5	0.051822	318.07815
6	0.054827	1456.59888
7	0.083160	6787.83588
8	0.099344	75803.58316
9	0.083345	3105960
10	0.105378	103861000
11	0.047853	8948410000
12	0.045569	1.31E+13
E_0 (MPa)	1733.89353	

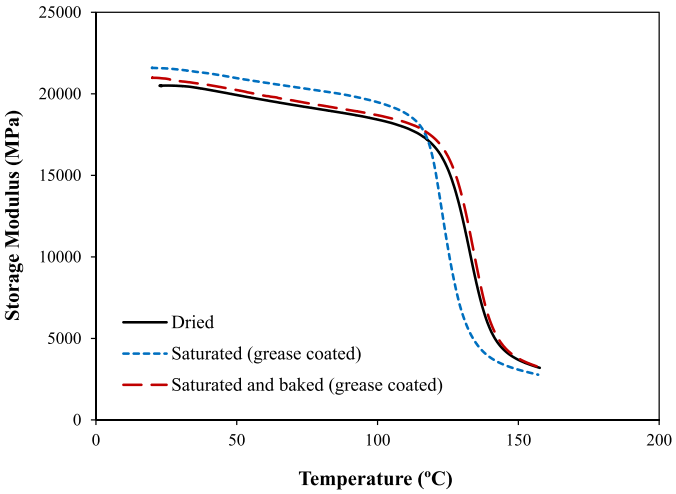

Fig. 12. Storage modulus curves of the dried, saturated, and baked (120 °C for 5 h) molding compound.

The characterization of relaxation behavior of moisture saturated molding compound is one of the most important objectives of this paper. As shown in Fig. 9, the sample is exposed to high temperatures for several hours during the stress relaxation test, therefore maintaining constant moisture concentration during test is a critical issue. In [13]–[15], the high thermal grease or epoxy adhesive had been coated on the sample surface to prevent moisture diffusion. To examine the moisture and high thermal grease effect on material behavior, preliminary DMA tests have been performed with three specimens: 1) dry sample; 2) grease coated saturated sample; and 3) grease coated saturate sample baked in an isothermal chamber at 120 °C for 5 h. A strain of 0.1% was applied with 1-Hz frequency in the three-point bending mode. The result is shown in Fig. 12. Assuming that the onset of large drop of storage modulus is T_g, the saturated status exhibits approximately 10 °C lower T_g than the dry condition. And the modulus increases about 6% in the saturated condition. The slope of baked specimen corresponds with dry specimen slope, which implies that the grease cannot capture the moisture inside the sample during test.

To explain the relaxation modulus change with respect to moisture loss in the simulation, a simple assumption

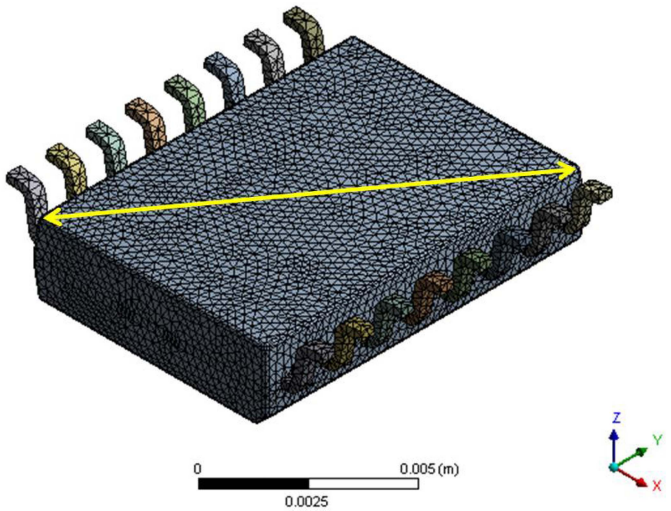

Fig. 13. FEA model and diagonal to obtain the out-of-plane deformation.

TABLE IV
MATERIAL PROPERTIES

Material		E (GPa)	CTE (ppm/°C)	ν
Silicon		163	2.6	0.22
Lead frame		129	16.6	0.34
Molding compound		Table 2	Fig. 8 (a)	0.29
Die attach adhesive		Table 3	Fig. 8 (b)	0.35
Seal glass	below 135 °C	50	7	0.29
	above 135 °C	40	15	0.44

was made. As shown in Fig. 12, the T_g decreased about 10 °C when the sample was saturated with moisture. Based on this observation, the relaxation test result of the dry sample was shifted. For instance, the relaxation behavior of dry sample at 100 °C was assumed to be the same with the saturated sample at 90 °C. However, the modulus change in DMA test in Fig. 12 was not considered in this assumption. Since this amount of discrepancy is usually observed due to sample alignment or other factors. This shift assumption will be further discussed in the following section.

IV. SIMULATION

A. Validation Study

Commercial FEA software, ANSYS 14.5, was utilized in this paper. Beginning with version 14, ANSYS is capable of simulating diffusion and related behaviors, such as hygroscopic swelling [23]. In [4], [7], [12], [23], and [24], the heat transfer analogy was used to predict moisture diffusion. Fig. 13 shows the FEA model used for these simulations. The element SOLID 226 and 227 were implemented to build the model. XYZ displacement of one edge node, YZ displacement of another edge node, and Z displacement of the other edge node on the top surface of the MEMS were constrained as a boundary condition to remove rigid body motions. Since the temperature of the PMC process was 175 °C, it was determined to be the reference temperature (no deformation temperature or stress free temperature). Material properties are listed in Table IV. Except for the molding compound and the die attach adhesive, material properties were obtained from the literatures. For the validation of simulation, the out-of-plane

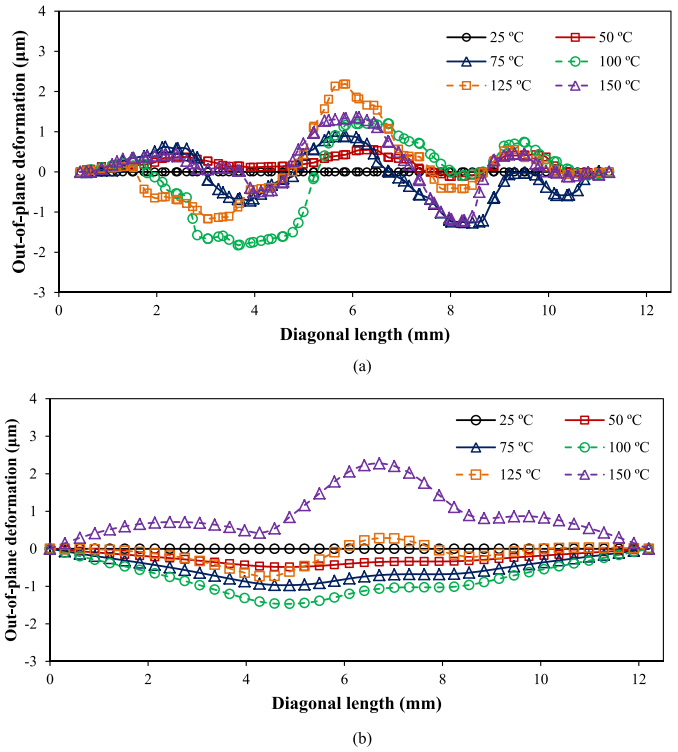

Fig. 14. Comparison of out-of-plane deformation between the test data and FEA results. (a) Experimental result. (b) Simulation result.

deformation of MEMS sensor device was measured by DIC and compared with the simulation result. The simulation model was cooled from 175 °C to 25 °C. The relative deformation to 25 °C was analyzed to remove the effect of cure shrinkage. This approach is valid because the focus of this paper is the relative stress comparison and the cure shrinkage is an additional deformation and constant through the temperature change [10]. The out-of-plane deformation data were extracted from the diagonal of the bottom surface, which is the side closer to both the MEMS and ASIC dies (Fig. 13). The result is plotted in Fig. 14. The simulation results did not identically match the experiment due to the infinitesimal amount of deformation. However, it has been confirmed that the out-of-plane deformation range over the temperature can be accurately predicted by simulation. In addition, the FEA stress and displacement data were imported to the MEMS sensor and package interaction (MPI) simulations at Analog Devices, Inc. (ADI). The result of MPI was internally validated with device offset.

B. Temperature Cycle With Moisture Effect

To evaluate the effect of moisture on the MEMS device under stress, temperature cycling was simulated. After the sample was cooled to 25 °C from 175 °C (stress free temperature), it absorbed moisture and reached the saturated condition. Then, the sample went through the temperature cycling in which moisture desorption process occurred simultaneously. The saturated concentration (C_{sat}) of 0.004 mg/mm^3 measured at the 85 °C/85% RH condition was also utilized for 25 °C. It has been discussed that there is no strong

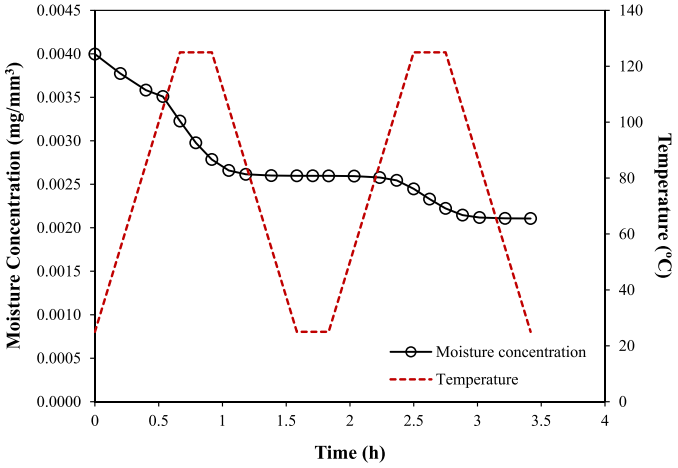

Fig. 15. Moisture desorption during the temperature cycling.

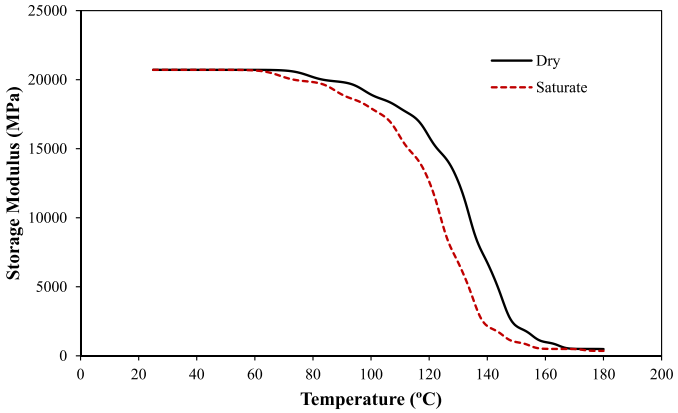

Fig. 16. T_g shift by changing the reference temperature of the shift function (1-Hz test frequency).

relationship between saturated concentration and temperature below 100 °C [24]. Each cycle consists of ramp up and ramp down processes with a rate of 2.5 °C/min, 125 °C dwelling for 15 min, and 25 °C dwelling process for 15 min. To implement the fully saturated condition at 25 °C in the simulation, the transient effect on diffusion field was turned OFF at 25 °C and the saturated condition was applied on the surface of the mold (fully saturated boundary condition). This step was solved to generate a fully saturated steady-state solution. After the model was saturated, the moisture concentration at the surface of mold was changed to zero (fully dried boundary condition) and the time integration on diffusion field was turned ON to include the transient effect of moisture diffusion. This is the first step of the desorption process. The transient effect on structural fields remained off during the whole simulation. The amount of moisture in the mold was calculated and plotted in Fig. 15. It is obvious that the desorption rate at high temperatures is much greater than at low temperatures. After two cycles, about a half of the moisture still remains in the molding compound.

While the CHS can be handled with ANSYS 14 or later version by inputting a material property called coefficient of diffusion expansion, taking the moisture impact on viscoelastic behavior is a more challenging issue in simulation. It has been observed that dry and moisturized mold compound behave differently in both the stress relaxation test [13]–[15] and

dynamic test (Fig. 16). Prior researchers have proposed the idea of time–water content superposition, trying to describe the relationship between moisture content and stress relaxation using shift functions such as WLF. Despite the efforts in experimental observation, this effect has not been adequately studied from a simulation/modeling perspective. In this paper, to illustrate the moisture impact on viscoelasticity, the T_g changed shift function was introduced. Instead of performing a series of stress relaxation tests, the new shift function was estimated for saturated sample based on the amount of T_g shifted from the DMA test. The storage modulus and loss modulus can be calculated from the Prony series by performing a Fourier transform [18]

$$E(\omega) = E_\infty + i\omega \sum_{i=1}^{n} \int_0^\infty E_i \exp(-i\omega t) dt. \tag{13}$$

By separating the real and imaginary parts, we obtain

$$E_s = E_0 \left(\alpha_\infty + \sum_{i=1}^{n} \frac{\alpha_i \tau_i^2 \omega^2}{1 + \tau_i^2 \omega^2} \right) \tag{14}$$

and

$$E_l = E_0 \sum_{i=1}^{n} \frac{\alpha_i \tau_i \omega}{1 + \tau_i^2 \omega^2} \tag{15}$$

where ω is the angular frequency, E_s and E_l are the storage and loss modulus, respectively. $\alpha_i = E_i / E_0$ is the normalized modulus in the Prony series. Therefore, if the reference temperature (T_0) is decreased in the WLF shift function (12) by ΔT_0 while C_1, C_2, and Prony series remain same, the stress relaxation curves would shift leftward by the corresponding amount in the logarithm time scale. In addition, the storage modulus and loss modulus will shift down in temperature exactly by ΔT_0. To demonstrate this effect, the modulus temperature curve (Fig. 16) was plotted for dry and saturated mold material by a theoretical calculation. It is clear that the T_g shift effect is very similar to the trend observed in experiments. Using the moisture data in Fig. 15, the shift function for the molding compound was changed in each load step

$$\log \alpha_T = -\frac{C_1 \{T - [T_0 - \Delta T_0(C)]\}}{C_2 + \{T - [T_0 - \Delta T_0(C)]\}}. \tag{16}$$

The amount of T_g shift (ΔT_0) was set proportionally to the amount of average moisture concentration. For the saturated condition, the shift of 10 °C was applied.

The moisture impact combined with viscoelasticity on MEMS stress during thermal cycles is shown in Fig. 17. Three different cases were compared: 1) a simple model with no moisture effect at all (viscoelasticity only); 2) a model considering both the viscoelasticity and hygroscopic effect; and 3) a model considering the viscoelasticity, hygroscopic swelling, and T_g shift. The normal stress in x-axis at the center node of the top surface of MEMS was plotted. The time with negative sign in x-axis is an arbitrary time before the temperature cycling is started. The initial point indicates the stress at 25 °C after the cool down process from 175 °C.

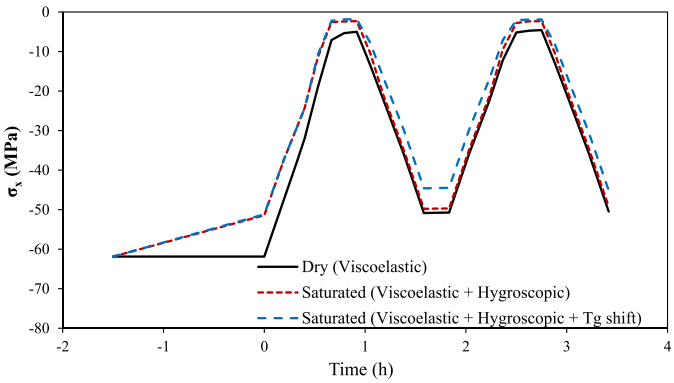

Fig. 17. MEMS stress during the temperature cycling.

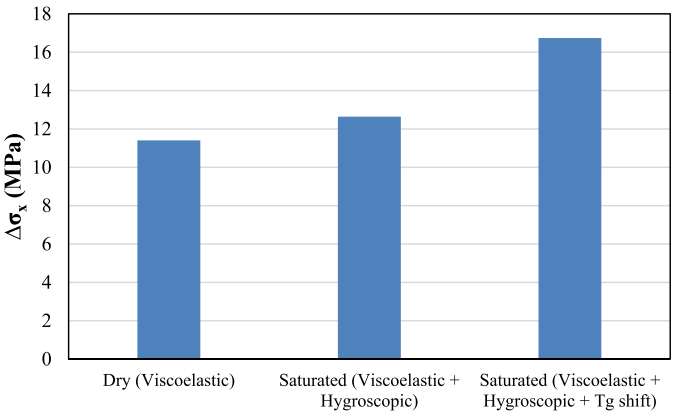

Fig. 18. MEMS stress change between the initial point and after temperature cycles.

The expansion of molding compound due to moisture absorption alleviates the compressive stress from the cool down process before temperature cycling. After temperature cycling, three notable phenomena can be observed. First, the compressive stress reduces in the temperature cycling due to the stress relaxation effect of molding compound. The most significant change happens in the first cycle. Second, the hygroscopic swelling behavior results in smaller compressive stress, yet the effect becomes less significant as the moisture is lost due to thermal cycling. Finally, when the T_g shift effect is considered, the stress change is greater. As a result, the stress after cycling is smaller.

This simulation result should give an indication of how much the MEMS device output deviates from its initial null output. Assuming that the starting points of the graph in Fig. 17 are the initial device outputs after the PMC process, more signal shift is generated with moisture after the temperature cycling than when only viscoelasticity is considered. The stress changes between the initial point and after two temperature cycles are shown in Fig. 18. This signal shift can be minimized by robust sensor design or proper packaging material selection.

V. Conclusion

The stresses of a moisture saturated MEMS sensor device subjected to temperature cycles have been analyzed. The moisture-dependent characteristics of molding compound were investigated. To measure CHS of molding compound, the

dimensional change of moisture saturated molding compound at various temperatures was observed using DIC method. In addition, the weight loss at the same condition was monitored by weight scale to determine diffusivity of water in the molding compound. The viscoelasticity of molding compound was characterized by stress relaxation test. To explain the moisture-induced viscoelastic behavior, a simple assumption was introduced based on T_g shift of DMA result. The results were utilized in the numerical simulation to evaluate MEMS stress. When the sample was saturated at 25 °C and subjected to temperature cycling, it has been demonstrated by the following.

1) The compressive stress reduces in the temperature cycling due to the stress relaxation effect of molding compound.
2) The hygroscopic swelling behavior results in smaller compressive stress.
3) When the T_g shift effect is considered, the stress change is greater so the stress calculated after temperature cycling was concluded to be the smallest.

Compared with the initial compressive stress after the PMC, a smaller stress generates a larger signal shift in the MEMS sensor device. Therefore, the result implies that a greater MEMS signal change occurs when the hygroscopic behavior affects the viscoelastic properties of the molding compound.

REFERENCES

[1] H. Ardebili, E. H. Wong, and M. Pecht, "Hygroscopic swelling and sorption characteristics of epoxy molding compounds used in electronic packaging," *IEEE Trans. Compon. Packag. Technol.*, vol. 26, no. 1, pp. 206–214, Mar. 2003.

[2] S. Yi, J. S. Goh, and J. C. Yang, "Residual stresses in plastic IC packages during surface mounting process preceded by moisture soaking test," *IEEE Trans. Compon., Packag., Manuf. Technol. B*, vol. 20, no. 3, pp. 247–255, Aug. 1997.

[3] E. Stellrecht, B. Han, and M. G. Pecht, "Characterization of hygroscopic swelling behavior of mold compounds and plastic packages," *IEEE Trans. Compon. Packag. Technol.*, vol. 27, no. 3, pp. 499–506, Sep. 2004.

[4] E. H. Wong, K. C. Chan, R. Rajoo, and T. B. Lim, "The mechanics and impact of hygroscopic swelling of polymeric materials in electronic packaging," in *Proc. 50th IEEE Electron. Compon. Technol. Conf. (ECTC)*, Las Vegas, NV, USA, May 2000, pp. 576–580.

[5] S. Park, H. Zhang, X. Zhang, S. L. Ng, and H. C. Lee, "Temperature dependency of coefficient of hygroscopic swelling of molding compound," in *Proc. 59th IEEE Electron. Compon. Technol. Conf. (ECTC)*, San Diego, CA, USA, May 2009, pp. 172–179.

[6] C. Jang, S. Yoon, and B. Han, "Measurement of the hygroscopic swelling coefficient of thin film polymers used in semiconductor packaging," *IEEE Trans. Compon. Packag. Technol.*, vol. 33, no. 2, pp. 340–346, Jun. 2010.

[7] J. B. Kwak, "Experimental assessment of electronic package deformation using optical full-field deformation measurement system," Ph.D. dissertation, Dept. Mech. Eng., Binghamton Univ., Binghamton, NY, USA, 2010.

[8] S. Park, D. Liu, Y. Kim, H. Lee, and S. Zhang, "Stress evolution in an encapsulated MEMS package due to viscoelasticity of packaging materials," in *Proc. IEEE 62nd Electron. Compon. Technol. Conf. (ECTC)*, May/Jun. 2012, pp. 70–75.

[9] R. H. Krondorfer and Y. K. Kim, "Packaging effect on MEMS pressure sensor performance," *IEEE Trans. Compon. Packag. Technol.*, vol. 30, no. 2, pp. 285–293, Jun. 2007.

[10] Y. Kim, H. Lee, X. Zhang, and S. Park, "Optimal material properties of molding compounds for MEMS package," *IEEE Trans. Compon., Packag., Manuf. Technol.*, vol. 4, no. 10, pp. 1589–1597, Oct. 2014.

[11] J. Keller *et al.*, "Effect of moisture swelling on MEMS packaging and integrated sensors," *Microelectron. Rel.*, vol. 53, nos. 9–11, pp. 1648–1654, 2013.

[12] S. Yoon, B. Han, S. Cho, and C.-S. Jang, "Non-linear finite element analysis for electronic packages subjected to combined hygroscopic and thermo-mechanical stresses," in *Proc. 7th Electron. Packag. Technol. Conf. (EPTC)*, vol. 2. Dec. 2005, pp. 569–574.

[13] A. Ishisaka and M. Kawagoe, "Examination of the time–water content superposition on the dynamic viscoelasticity of moistened polyamide 6 and epoxy," *J. Appl. Polym. Sci.*, vol. 93, no. 2, pp. 560–567, 2004.

[14] X. Ma, K. M. B. Jansen, and L. J. Ernst, "Moisture effects on the creep of thermosetting IC packaging polymers," in *Proc. 7th. Int. Conf. Thermal, Mech. Multiphys. Simulation Experim. Micro-Electron. Micro-Syst. (EuroSimE)*, Apr. 2006, pp. 1–5.

[15] S. Rzepka, R. Pantou, F. Bormann, B. Bramer, I. Brabandt, and B. Michel, "Toolbox for visco-elastic material modeling of smart lightweight structures," in *Proc. 14th Int. Conf. Thermal, Mech. Multi-Phys. Simulation Experim. Microelectron. Microsyst. (EuroSimE)*, Apr. 2013, pp. 1–8.

[16] P. Bhargava, K. C. Chuang, K. Chen, and A. Zehnder, "Moisture diffusion properties of HFPE-II-52 polyimide," *J. Appl. Polym. Sci.*, vol. 102, no. 4, pp. 3471–3479, Nov. 2006.

[17] J. E. Galloway and B. M. Miles, "Moisture absorption and desorption predictions for plastic ball grid array packages," *IEEE Trans. Compon., Packag., Manuf. Technol. A*, vol. 20, no. 3, pp. 274–279, Sep. 1997.

[18] J. D. Ferry, *Viscoelastic Properties of Polymers*, 3rd ed. New York, NY, USA: Wiley, 1980.

[19] C. Jang, B. Han, and S. Yoon, "Comprehensive moisture diffusion characteristics of epoxy molding compounds over solder reflow process temperature," *IEEE Trans. Compon. Packag. Technol.*, vol. 33, no. 4, pp. 809–818, Dec. 2010.

[20] H. Zhang, "Investigation of hygroscopic swelling behavior of molding compound and its impact on encapsulated MEMS packages," Ph.D. dissertation, Dept. Mech. Eng., Binghamton Univ., Binghamton, NY, USA, 2011.

[21] X. Chen, S. Zhao, and L. Zhai, "Moisture absorption and diffusion characterization of molding compound," *ASME J. Electron. Packag.*, vol. 127, no. 4, pp. 460–465, 2005.

[22] S. B. Park, R. Dhakal, and R. Joshi, "Comparative analysis of BGA deformations and strains using digital image correlation and Moiré interferometry," in *Proc. SEM Annu. Conf. Expo. Experim. Appl. Mech.*, Portland, OR, USA, Jun. 2005, pp. 1–8.

[23] D. Liu and S. Park, "A note on the normalized approach to simulating moisture diffusion in a multimaterial system under transient thermal conditions using ANSYS 14 and 14.5," *J. Electron. Packag.*, vol. 136, no. 3, p. 034501, 2014.

[24] C. Jang, S. Park, S. Yoon, and B. Han, "Advanced thermal-moisture analogy scheme for anisothermal moisture diffusion problem," *J. Electron. Packag.*, vol. 130, no. 1, p. 011004, Mar. 2008.

[25] J. Zhou, S. P. Lahoti, M. P. Sitlani, S. C. Kallolimath, and R. Putta, "Investigation of nonuniform moisture distribution on determination of hygroscopic swelling coefficient and finite element modeling for a flip chip package," in *Proc. EuroSimE*, Apr. 2005, pp. 112–119.

[26] J. Zhou, "Analytical and numerical bound analysis of hygroscopic swelling characterization," in *Proc. 56th Electron. Compon. Technol. Conf. (ECTC)*, 2006, pp. 734–739.

[27] J. Zhou, T. Y. Tee, and X. J. Fan, "Hygroscopic swelling of polymeric materials in electronic packaging: Characterization and analysis," in *Moisture Sensitivity of Plastic Packages of IC Devices*, X. J. Fan and E. Suhir, Eds. New York, NY, USA: Springer-Verlag, 2010, ch. 7, pp. 153–179.

[28] X. Fan and J.-H. Zhao, "Moisture diffusion and integrated stress analysis in encapsulated microelectronics devices," in *Proc. 12th. Int. Conf. Thermal, Mech. Multiphys. Simulation Experim. Microelectron. Microsyst. (EuroSimE)*, Linz, Austria, 2011, pp. 1/8–8/8.

Yeonsung Kim received the B.S. and M.S. degrees in mechanical engineering from Chung-Ang University, Seoul, Korea, in 2002 and 2004, respectively, and the Ph.D. degree in mechanical engineering from the State University of New York at Binghamton, Binghamton, NY, USA, in 2014.

He joined Samsung Electronics Company, Ltd., Suwon, Korea, in 2004, where he was involved in evaluating and improving the reliability of electronic packaging for mobile devices for four and a half years. He is currently a Packaging and Assembly Engineer with Analog Devices, Inc., Wilmington, MA, USA, where he is involved in a packaging development for microelectromechanical systems.

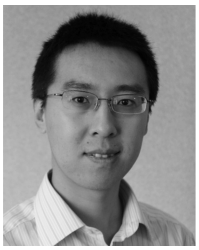

Dapeng Liu received the bachelor's degree in mechanical engineering from the Harbin Institute of Technology, Harbin, China, in 2009. He is currently pursuing the Ph.D. degree with the Opto-Mechanics and Physical Reliability Laboratory, Department of Mechanical Engineering, State University of New York at Binghamton, Binghamton, NY, USA.

His current research interests include computational modeling, stress analysis, microelectromechanical systems packaging, and 3-D integration using through-silicon-via technology.

Hohyung Lee received the B.S. degree in industrial system engineering and the M.S. degree in mechanical engineering from the State University of New York at Binghamton, Binghamton, NY, USA, where he is currently pursuing the Ph.D. degree with the Opto-Mechanics and Physical Reliability Laboratory, Department of Mechanical Engineering.

Ruiyang Liu received the B.S. degree in materials engineering from the Harbin Institute of Technology, Harbin, China, in 2012. She is currently pursuing the Ph.D. degree in mechanical engineering with the State University of New York at Binghamton, Binghamton, NY, USA.

Her current research interests include experiments and simulation to improve the reliability of microelectronics/microelectromechanical systems packaging.

Dipak Sengupta received the B.Tech. degree in metallurgical engineering from IIT Kharagpur, Kharagpur, India, and the M.S. degree in materials science from the State University of New York at Stony Brook, Stony Brook, NY, USA.

He was a Senior Materials Engineer with Honeywell, Morristown, NJ, USA. He has developed various package technologies and associated assembly processes with Analog Devices Inc., Wilmington, MA, USA, for the past 28 years. He is responsible for leading development and implementation of new semiconductor package technology and also manages university relations and the patent process with the Manufacturing Group, Analog Devices Inc. He has over 20 technical publications, including six U.S. patents and several pending. His current research interests include package development for high performance microelectromechanical systems devices.

Mr. Sengupta received the H. W. Sweatt Award, which is Honeywell's highest award for technical achievement.

Seungbae Park received the Ph.D. degree from Purdue University, West Lafayette, IN, USA, in 1994.

He was with IBM, Armonk, NY, USA, as a Development and Reliability Engineer, where he was responsible for flip chip technology. Since 2002, he has been teaching with the Department of Mechanical Engineering, State University of New York at Binghamton, Binghamton, NY, USA, as a Professor. He has over 100 technical publications and holds four U.S. patents. His current research interests include physical reliability for microelectronics and microelectromechanical systems packaging.

Dr. Park has served for many technical communities, such as the Chair of the iNEMI's Modeling and Simulation Technical Work Group of the Electronics Packaging Council in the Society of Experimental Mechanics, a Reliability Committee Member of ECTC, and an Associate Editor of the *ASME Journal of Electronic Packaging*.